NEW QUALITY REPRESENTATION FOR HYPERSPECTRAL IMAGES

Emmanuel Christophe[†], Dominique Léger[‡], and Corinne Mailhes[*]

[†] CNES DCT/SI/AP Bpi 1219, 18 av E. Belin 31401 Toulouse Cedex 09
emmanuel.christophe@cnes.fr
[‡] Optics Department of ONERA, 2 avenue E. Belin BP 4025, 31055 Toulouse Cedex 4
[*] University of Toulouse, TESA - IRIT - ENSEEIHT, 14 port St Etienne 31000 Toulouse, FRANCE

Commission VII/3

ABSTRACT:

Assessing the quality of a hyperspectral image is a difficult task. However, this assessment is required at different levels of the instrument design: evaluation of the signal to noise ratio necessary for a particular application, determining the acceptable level of losses from compression algorithms for example. It has been shown previously that a combination of five quality criteria can provide a good evaluation of the impact of some degradation on applications, such as classification algorithms for example. This paper refines this concept, providing a representation of the degradation which allows predicting the impact on applications.

1 INTRODUCTION

Quality criteria should be easily applicable to measure the loss of information caused by compression or by any other forms of processing. In the case of ordinary 2D images, a quality criterion has often to reflect the visual perception of a human observer. This is not the case for hyperspectral images, which are first aimed to be used through classification or detection algorithms. Therefore, quality criteria have to be relevant to these corresponding applications. For example, some papers ([Ryan and Arnold, 1997], [Hu et al., 2004], [Qian, 2004]) address the problem of evaluating compression impact on specific hyperspectral applications. However, quality evaluations within the context of specific applications are heavy to conduct as they require in-depth knowledge of these applications.

In a previous work [Christophe et al., 2005], different degradations were applied to hyperspectral images: additive white noise, smoothing (spectral and/or spatial) with a lowpass filtering of the data, Gibbs effect (ringing around sharp changes) and JPEG 2000 compression [Taubman and Marcellin, 2002] using a multicomponent transform. Different images from the NASA/JPL AVIRIS hyperspectral airborne sensor were used for the experiments (Fig. 1). Finally, five quality criteria have been selected to give a valuable representation of the degradations affecting the hyperspectral data and their impacts on three different classification algorithms. These five quality criteria were found to be a good combination to discriminate between data degradation and appear to be almost orthogonal to each other. One advantage of this combination is the mix between local and global criteria for both spatial and spectral dimensions, thus enabling the detection of local and global degradations.

However, the way to use these measures was not detailed. The present paper proposes in the following section a graphic representation of the chosen quality criteria. A numerical method is then derived in section 3 from this representation to provide a way to identify the degradation nature if unknown and to predict its impact on a specific application. The interest of the proposed representation is finally illustrated and compared with traditional SNR-based measure.
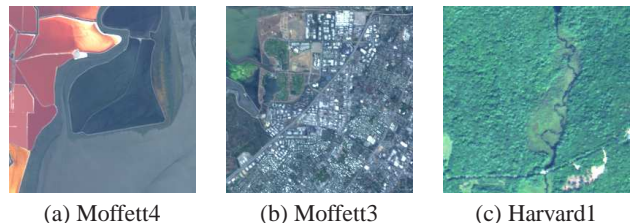

(a) Moffett4   (b) Moffett3   (c) Harvard1

Figure 1: Different hyperspectral images used during the experiments. (a) and (b) are different parts from the f970620t01p02_r03 run from AVIRIS sensor on Moffett Field site. (a) presents uniform spatial area with strong spectral features. (b) is mixed area with city (strong spatial frequency features). (c) is from the f010903t01p01_r03 AVIRIS run over Harvard Forest, it contains mostly vegetation whose spectrum contrasts with man-made objects.

2 QUALITY REPRESENTATION

2.1 Efficient representation for five criteria

The five quality criteria retained in [Christophe et al., 2005] were the MAD, MAE, RRMSE, F_λ and $Q_{(x,y)}$. Denoting $I(x, y, \lambda)$ the original image, $\widetilde{I}(x, y, \lambda)$ the degraded image and $e_{\widetilde{I}} = I - \widetilde{I}$ (x, y being spatial dimensions and λ the spectral one), these five quality criteria are defined as

- Maximum Absolute Difference

$$\text{MAD} = \mathcal{L}_\infty(I - \widetilde{I}) = \max_{(x,y,\lambda)} \left\{ \left| e_{\widetilde{I}}(x, y, \lambda) \right| \right\}. \quad (1)$$

- Mean Absolute Error

$$\text{MAE} = \frac{\mathcal{L}_1(I - \widetilde{I})}{n_x n_y n_\lambda} = \frac{1}{n_x n_y n_\lambda} \sum_{x,y,\lambda} \left| e_{\widetilde{I}}(x, y, \lambda) \right|. \quad (2)$$

where n_x, n_y and n_λ are the number of pixels for each dimension.

- Relative RMSE

$$\text{RRMSE} = \sqrt{\frac{1}{n_x n_y n_\lambda} \sum_{x,y,\lambda} \left(\frac{e_{\widetilde{I}}(x,y,\lambda)}{I(x,y,\lambda)} \right)^2}. \quad (3)$$

Note that, as the RRMSE enhances the importance of errors on small values, it is important to consider the particular case of values below the sensor noise. Small values of $I(x,y,\lambda)$ can be considered as random and are ignored for the computation of the RRMSE.

- Spectral Fidelity [Eskicioglu and Fisher, 1995]

$$F_\lambda = \min_{(x,y)} \left\{ F\left(I(x,y,\cdot), \widetilde{I}(x,y,\cdot) \right) \right\}. \quad (4)$$

with

$$F(U,V) = 1 - \frac{\mathcal{L}_2^2(U-V)}{\mathcal{L}_2^2(U)}. \quad (5)$$

- $Q_{(x,y)}$ [Wang and Bovik, 2002]

$$Q_{(x,y)} = \min_\lambda \left\{ Q\left(I(\cdot,\cdot,\lambda), \widetilde{I}(\cdot,\cdot,\lambda) \right) \right\}. \quad (6)$$

with

$$Q(U,V) = \frac{4\,\sigma_{UV}\,\mu_U\,\mu_V}{(\sigma_U^2 + \sigma_V^2)(\mu_U^2 + \mu_V^2)} \quad (7)$$

where σ_{UV} is the covariance between U and V.

All these criteria measure a distance between an original image and a degraded version of this image.

Representing a combination of five values is a challenge and working on a five-dimensional plot would not enable efficient assessment. A good way to represent these values is to use a star diagram (Fig 2) which gives a more intuitive vision than a classical x-y representation in this case. The five axes of the diagram correspond to the five quality criteria. Scale for all the figures in this paper are the same. For MAD, MAE and RRMSE, origin corresponds to 0 (no degradation). The extremity of the axes corresponds to value 5000 for MAD, 40 for MAE and 0.1 for RRMSE. For F_λ and $Q_{(x,y)}$, origin corresponds to 1 (no degradation), extremity being 0.9 for F_λ and 0.6 for $Q_{(x,y)}$. These values were found to provide a good differentiation between different degradations. These specific values are important for visualization and comparison, they are not important by themselves, it is just necessary to use the same scales on the different figures. The shape of the diagram is characteristic of the degradation as seen in figures 2, 3 and 4.

Parameters for the degradation are presented in [Christophe et al., 2005]. Basically, this is the variance for the white noise, the filter size for the smoothing, the scale factor for the Gibbs filter, and the compression rate for JPEG 2000.

2.2 Shape characterizes the degradation

This representation is robust relatively to the amplitude of the degradation. The shape is similar for a given degradation; the degradation pattern is inflated when the degradation level increases (Figs. 2-4). For example in Fig. 2, the innermost shape (green) corresponds to a white noise with a low variance. When the noise variance increases, the quality decreases and the quality diagram dilates.
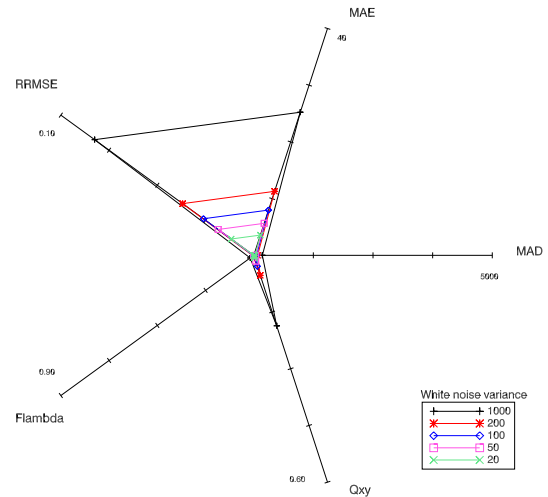

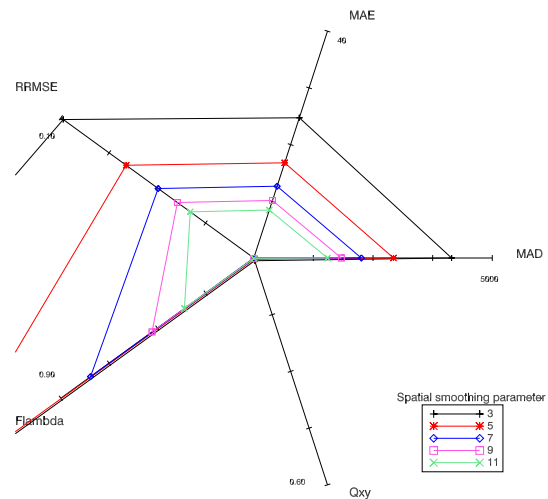Figure 2: Quality for different values of additive white noise on *moffett4* image.

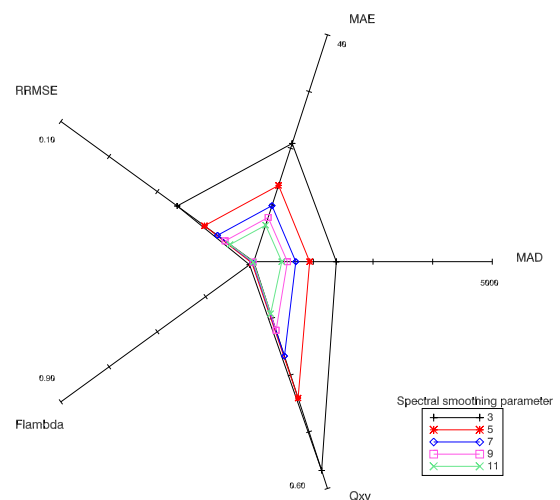Figure 3: Quality for different values of spatial smoothing on *moffett4* image.

Figure 4: Quality for different values of spectral smoothing on *moffett4* image.

To be valuable, this representation has to report accurately the quality of the image and the performance that one can expect from a particular application whatever the image is. However, most degradation effects are sensitive to the image. It is easy to understand that a spatial smoothing will have a greater influence on a city image than on a uniform area (Fig. 7).
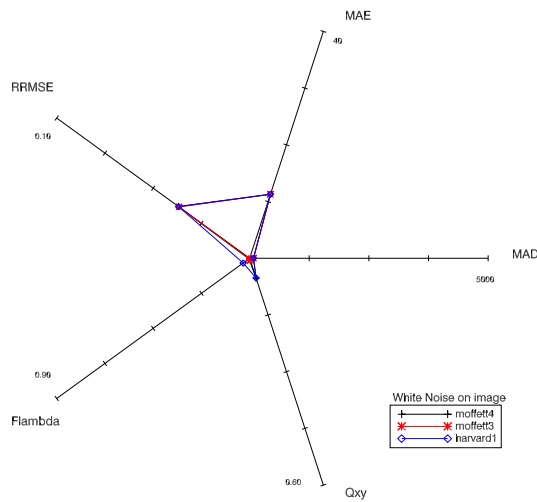

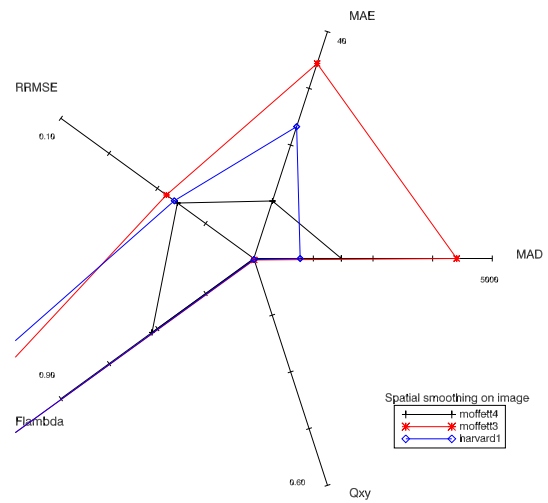Figure 5: Quality for different values of white noise on three different images.

Figure 7: Quality for different values of spatial smoothing on three different images.
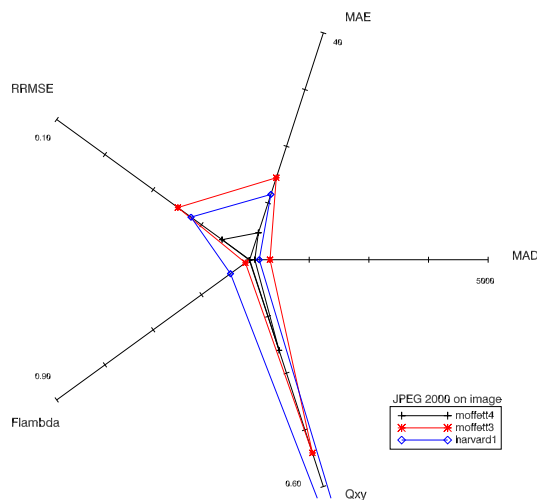

Figure 6: Quality for different rates for JPEG 2000 on three different images.

When considering spectral smoothing, the same conclusion holds. *Moffett3* and *harvard1* images have more high frequency components than *moffett4*. The spectral content of *harvard1* is completely different from *moffett3* and *moffett4*. Thus, the quality figures differ (Fig. 8). However, as we can expect the influence of the smoothing on applications to be different also, this is not surprising.

It is important to notice that the representation is quite robust for the three different images *moffett3*, *moffett4* et *harvard1* for the white noise and JPEG 2000 degradations (Figs. 5 and 6).

3 QUANTITATIVE EVALUATION

3.1 Distance between degradations

The ideal situation to reach, the *Grail* of the quality criteria would be to infer precisely the degradation impact on application know-
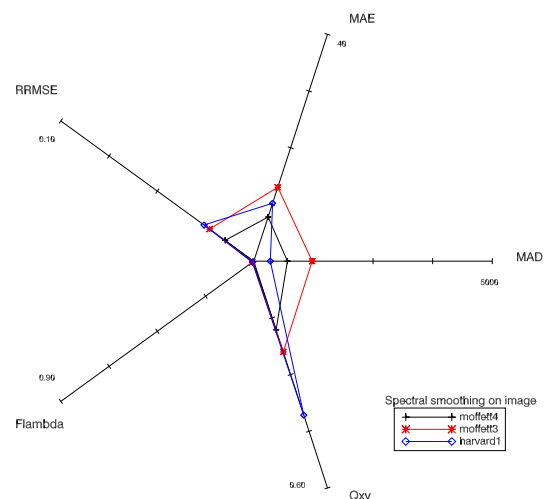
Figure 8: Quality for different values of spectral smoothing on three different images.

ing only the five values of the criteria and a link for one image between the five values and the impact for a given application.

It is possible to define a validation protocol for the previous representation at different levels (each being more difficult). We assume that we know the quality criteria values corresponding to several degradations for few levels (e.g. Fig. 2-4). We also know the impact on one application (SAM classification in our case) of these degradations on the results. We can now try to predict the impact for

- a known degradation but with a different level on the same image (first situation);

- an unknown degradation on the same image (second situation);

- an unknown degradation on a different image (third situation).

It has to be highlighted that the choice of the SAM classification is not determinant and is chosen only for demonstration purpose. Any other hyperspectral application giving a quantifiable result could have been used.

In the following part, results obtained on *moffett3* image are used. Only one image is used as a reference as it is not easy to obtain applications results for different images (it is precisely the reason why quality criteria are important). In the situation where another image is required, *moffett4* is used.

When we are confronted to an unknown situation, we will try to find the nearest known diagram. To be able to find the *nearest* diagram, we need to define a *distance*. A Euclidean distance, in this five-dimensional space, is the most intuitive solution.

We are still confronted to the problem of the scale between criteria: the MAD variation domain, which can easily reach 2000, has nothing in common with the variation domain of F_λ, which is kept between 0.9 and 1. There is no ideal solution to this problem so we decide to normalize arbitrarily the values using the same scales as on the previous diagrams. We denote as $\widetilde{\cdot}$ this normalized value.

Thus, the distance between two diagrams is defined as:

$$d = \sqrt{\widetilde{\Delta^2_{\mathrm{MAD}}} + \widetilde{\Delta^2_{\mathrm{MAE}}} + \widetilde{\Delta^2_{\mathrm{RRMSE}}} + \widetilde{\Delta^2_{F_\lambda}} + \widetilde{\Delta^2_{Q_{(x,y)}}}}. \quad (8)$$

The lower the distance, the more similar the two degradations. We now need to check if this distance performs well in the three situations described above.

3.2 Changing the degradation level (1st situation)

In the case where a white noise with a variance of 150 is applied to the image, let us compute the distance (8) to known degradations on the same image. Results are presented in table 1. Smallest distances are highlighted in bold and correspond to those with the white noise with a variance of 200 and the white noise with a variance of 100 (Tab. 1). In this situation, we can accurately predict the impact of the degradation on the application. We can infer a number of misclassified pixels between 163 and 255, which is correct: the real value is 222 (of the 65536 pixels in total).

Table 1: Distances for a white noise of variance 150.

Degradation type	Deg. param.	Distance	# of misclass.
White noise	50	0.169285	112
White noise	**100**	**0.0735083**	**163**
White noise	**200**	**0.0619829**	**255**
White noise	1000	0.634494	634
Spectral smoothing	3	1.57091	262
Spectral smoothing	5	0.917740	166
Spectral smoothing	7	0.627584	123
Spatial smoothing	13	1.40636	4248
Spatial smoothing	15	1.11240	3778
Mixed smoothing	11	1.90406	4881
Gibbs	50	0.195913	698
Gibbs	100	0.258957	425
JPEG 2000	0.5	0.857591	450
JPEG 2000	1.0	0.503311	142

The same accuracy is also observed when using this distance for other degradations. For example, in the case of spectral smoothing (Tab. 2) with an attenuation parameter of 4, the smallest distances correspond to the spectral smoothing with the parameters 3 and 5, which gives a number of misclassified pixels between 166 and 262 (the real value is 207).

Table 2: Distances for a spectral smoothing with an attenuation parameter of 4.

Degradation type	Deg. param.	Distance	# of misclass. pixels (SAM)
White noise	50	1.31986	112
White noise	100	1.40968	163
White noise	200	1.60283	255
White noise	1000	2.83994	634
Spectral smoothing	**3**	**0.365524**	**262**
Spectral smoothing	**5**	**0.271982**	**166**
Spectral smoothing	7	0.567515	123
Spatial smoothing	13	1.55253	4248
Spatial smoothing	15	1.35135	3778
Mixed smoothing	11	1.76783	4881
Gibbs	50	1.18216	698
Gibbs	100	1.22852	425
JPEG 2000	0.5	1.01159	450
JPEG 2000	1.0	0.931696	142

3.3 Unknown degradation (2nd situation)

In this second situation, let us consider some unknown degradation on *moffett3* image. The above examples (Tab. 1) show that, when dealing with the same image, the smallest distance is able to identify the degradation nature. To reinforce this, we remove the JPEG 2000 degradation from the known situations to be able to consider it as an unknown situation and find the nearest degradation to infer the number of misclassified pixels.

Distances are presented in table 3. The degradation caused by JPEG 2000 compression at 1 bit per pixel per band (bpppb) is identified as a mixture of a white noise with a variance of 100 and a spectral smoothing with an attenuation of 7. This identification corresponds to the intuitive one, looking at the diagram shape and considering the well-known effects of JPEG 2000. The predicted numbers of misclassified pixels are 163 and 123. The real value is 142. However, given the available possible prediction in the table, we can notice that the diagram distance managed to select some the closest values to the right answer to give a rough prediction.

3.4 Different images (3rd situation)

In this case, we use results obtained on *moffett3* to infer the likely degradation on *moffett4*. In the case of a white noise with a variance of 100, the distance between diagrams properly identifies the degradation as a white noise (Tab. 4). The distance interprets a white noise with a variance of 100 on *moffett4* as having the same effect than a white noise of variance 100 on *moffett3*. The predicted value of misclassified pixels is 163 whereas the real number is 91.

Table 3: Distance for JPEG 2000 at 1 bpppb.

Degradation type	Deg. param.	Distance	# of misclass.
White noise	50	0.493597	112
White noise	**100**	**0.492287**	**163**
White noise	200	0.520257	255
White noise	1000	0.884674	634
Spectral smoothing	3	1.26847	262
Spectral smoothing	5	0.634936	166
Spectral smoothing	**7**	**0.376314**	**123**
Spatial smoothing	13	1.50541	4248
Spatial smoothing	15	1.22905	3778
Mixed smoothing	11	1.91304	4881
Gibbs	50	0.505195	698
Gibbs	100	0.510643	425

Table 4: Distance for a white noise of variance 100 on *moffett4* image with degradation on *moffett3*.

Degradation type	Deg. param.	Distance	# of misclass.
White noise	50	0.107652	112
White noise	**100**	**0.0435569**	**163**
White noise	200	0.139344	255
White noise	1000	0.705412	634
Spectral smoothing	3	1.56918	262
Spectral smoothing	5	0.908723	166
Spectral smoothing	7	0.608943	123
Spatial smoothing	13	1.42293	4248
Spatial smoothing	15	1.12790	3778
Mixed smoothing	11	1.91772	4881
Gibbs	50	0.159746	698
Gibbs	100	0.198265	425
JPEG 2000	0.5	0.830507	450
JPEG 2000	1.0	0.449398	142

Table 5: Distance for JPEG 2000 at 0.5 bpppb on *moffett4* image with degradation on *moffett3*.

Degradation type	Deg. param.	Distance	# of misclass.
White noise	50	0.400136	112
White noise	100	0.419496	163
White noise	200	0.478324	255
White noise	1000	0.920144	634
Spectral smoothing	3	1.38425	262
Spectral smoothing	5	0.738476	166
Spectral smoothing	7	0.455491	123
Spatial smoothing	13	1.50678	4248
Spatial smoothing	15	1.22396	3778
Mixed smoothing	11	1.93958	4881
Gibbs	50	0.424221	698
Gibbs	100	0.407225	425
JPEG 2000	0.5	0.565506	450
JPEG 2000	**1.0**	**0.129164**	**142**

We also apply the method for a JPEG 2000 compression on *moffett4* at a bitrate of 0.5 bpppb. Distances are presented on table 5. The distance successfully identifies the degradation as being JPEG 2000. The *moffett4* image is more uniform, thus easier to compress. This property explains that degradations on *moffett4* for a bitrate of 0.5 bpppb are similar to those on *moffett3* at 1.0 bpppb. The number of misclassified pixels estimated by this method is 142, the real value being 82. There is a lack of reliability in this situation.

In the situation where the method is applied to a different image, it is difficult to evaluate precisely the impact of the degradation on the application. However, this method successfully identifies the nature of the degradation caused to the image. It would be worthwhile to detail these results on a greater number of images and applications.

3.5 Interest compared to traditional SNR

SNR, as well as MSE or PSNR, which are derived measures, do not reveal the nature of the degradation and do not allow inferring the impact on applications. This fact is illustrated on figure 9. Diagrams are plotted for different degradations leading to the same SNR. The five degradations are applied to the *moffett3* image to provide a SNR equal to 30 dB. We can clearly see from the diagram that even if these degradations led to the same SNR, their characteristics are completely different.

For the same image using only the SNR to measure the quality (here for a SNR of 30 dB), we cannot make the difference between

- a white noise with a variance of 2000: 1054 misclassified pixels;

- a spectral smoothing with an attenuation parameter of 4: 207 misclassified pixels;

- a spatial smoothing with an attenuation parameter of 15: 3778 misclassified pixels;
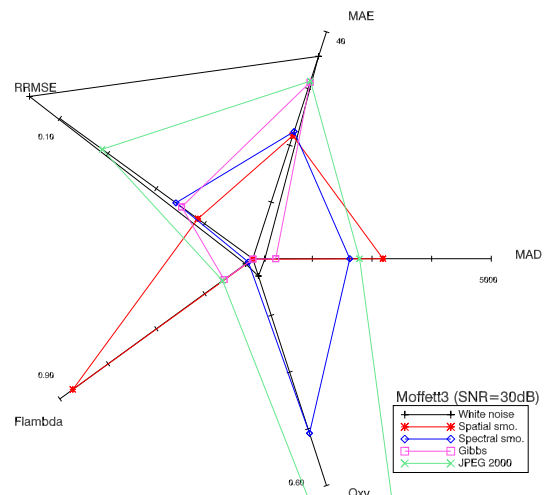

Figure 9: Quality for the 5 types of degradation giving the same SNR on *moffett3* image (30 dB).

- a Gibbs phenomenon with a parameter 20: 2029 misclassified pixels;

- a JPEG 2000 compression at the rate of 0.2 bpppb: 1772 misclassified pixels.

These degradations, all giving a SNR of about 30 dB, have an impact on the application varying from 207 to 3778 misclassified pixels. The SNR fails to give an estimation of the degradation impact on the hyperspectral image quality for the user, whereas the proposed use of the five criteria would allow to obtain it.

4 PERSPECTIVES

Results presented here are promising, given the possibility of degradation identification and impact evaluation on future applications. However, these results need to be confirmed on a bigger test basis with more images and especially more applications.

The five quality criteria are used here simply to define a distance relation. This simple method already gives promising results. It would be worthwhile to refine this using different method: e.g., using these five criteria as an entry for a neural network with the number of misclassified pixels as an output. *Support Vector Machine* (SVM) could also be a good candidate.

5 ACKNOWLEDGEMENT

REFERENCES

Christophe, E., Léger, D. and Mailhes, C., 2005. Quality criteria benchmark for hyperspectral imagery. IEEE Transactions on Geoscience and Remote Sensing 43(09), pp. 2103–2114.

Eskicioglu, A. M. and Fisher, P. S., 1995. Image quality measures and their performance. IEEE Transactions on Communications 43(12), pp. 2959–2965.

Hu, B., Qian, S.-E., Haboudane, D., Miller, J. R., Hollinger, A. B., Tremblay, N. and Pattey, E., 2004. Retrieval of crop chlorophyll content and leaf area index from decompressed hyperspectral data: the effects of data compression. Remote Sensing of Environment 92, pp. 139–152.

Qian, S.-E., 2004. Hyperspectral data compression using a fast vector quantization algorithm. IEEE Transactions on Geoscience and Remote Sensing 42(8), pp. 1791–1798.

Ryan, M. J. and Arnold, J. F., 1997. Lossy compression of hyperspectral data using vector quantization. Remote Sensing of Environment 61, pp. 419–436.

Taubman, D. S. and Marcellin, M. W., 2002. JPEG2000 Image Compression Fundamentals, Standards and Practice. Kluwer Academic Publishers, Boston, MA.

Wang, Z. and Bovik, A. C., 2002. A universal image quality index. IEEE Signal Processing Letters 9(3), pp. 81–84.